

## Establishment of a Novel Model of Peritoneal Carcinomatosis of the Peritoneal Extension Type

MOTOHIRO IMANO<sup>1,2</sup>, TATSUKI ITOH<sup>3</sup>, TAKAO SATOU<sup>3</sup>, AKIRA KIDO<sup>4</sup>, MASAHIRO TSUBAKI<sup>5</sup>,  
ATSUSHI YASUDA<sup>1</sup>, HIROAKI KATO<sup>1</sup>, HARUHIKO IMAMOTO<sup>1</sup>, SHOZO NISHIDA<sup>5</sup>,  
HIROSHI FURUKAWA<sup>1</sup>, YOSHIFUMI TAKEYAMA<sup>1,2</sup>, KIYOKATA OKUNO<sup>1</sup> and HITOSHI SHIOZAKI<sup>1</sup>

Departments of <sup>1</sup>Surgery and <sup>3</sup>Pathology, Kinki University Faculty of Medicine, Osaka-Sayama, Osaka, Japan;

<sup>2</sup>Cancer Center, Kinki University Hospital, Osaka-Sayama, Osaka, Japan;

<sup>4</sup>Department of Orthopedic Surgery, Nara Medical University, Kashihara, Nara, Japan;

<sup>5</sup>Division of Pharmacotherapy, Kinki University Faculty of Pharmacy, Higashi-Osaka, Osaka, Japan

**Abstract.** Aim: Patients with scirrhous carcinoma of the gastrointestinal tract frequently develop peritoneal carcinomatosis—particularly of the peritoneal extension type (PET), which has a bad prognosis. We developed a novel animal model, suitable for testing treatments for PET. Material and Methods: In order to develop the model, we scraped the entire peritoneum of Fischer 344 rats with sterile cotton swabs and injected  $1 \times 10^6$  cells of the RCN-9 cell type into the peritoneal cavity. Results: In the novel experimental model, RCN-9 cells adhered only to the exposed basement membrane. The submesothelial layer and fibroblasts in the submesothelial layer grew and increased to a maximum at day 7, then decreased during late-phase peritoneal carcinomatosis. At day 14, RCN-9 cells coated the peritoneum in a manner similar to PET. Conclusion: We successfully established a novel animal model of peritoneal carcinomatosis that mimics clinicopathological features of PET. Fibroblasts in the submesothelial layer potentially play an important role in peritoneal carcinomatosis.

The locoregional progression of gastrointestinal and ovarian cancer frequently results in peritoneal carcinomatosis (PC), which is associated with poor prognosis and a median survival of less than six months (1, 2). Frequently, PC develops in cases of scirrhous carcinoma (SC), leading to more pessimistic prognoses (3, 4). In contrast to other macroscopic types, PC that originates from the gastrointestinal tract SC frequently

occurs as peritoneal extension type (PET) (3, 5). Therefore, the prognosis for PC of PET is worse compared with other macroscopic types of PC (5).

PET is currently treated with systemic chemotherapy with palliative, not curative intent (6), and a treatment modality for PET is not yet established. Therefore, we developed an animal model for testing the suitability of PET treatment modalities.

One requirement for an animal model of PET that we considered, was the selection of cancer cells that would coat the peritoneum in a manner similar to tumors. In earlier experimental animal models of PC, including mouse and rat models, PC lesions appeared as tumor nodules, which were present in the omentum, liver hilum, mesentery, diaphragm and the subcutaneous tissue, but not the peritoneum (7, 8). Thus, these models were not appropriate for investigating PET; development of a suitable experimental animal model was warranted.

The colonic adenocarcinoma cell line RCN-9 is the dimethylhydrazine-induced colon carcinoma of Fischer 344 rats (9). After RCN-9 cells were injected either subcutaneously or into the cecal subserosa of Fisher 344 rats, tumors reportedly exhibited progressive growth and metastasized to the lung (63.6%) and liver (40.0%) (9); treatment with both 5-fluorouracil and adriamycin gave an *in vivo* antitumor effect against RCN-9 cells. Song *et al.* also reported RCN-9 cells to be refractory to FS-7-associated-surface antigen (Fas) receptor-mediated apoptosis (10). These results show that the RCN-9 cell line is potentially suitable both as a model to study the mechanisms of metastasis and as a model for chemotherapeutic studies of metastatic disease. Furthermore, RCN-9 cells injected into peritoneal cavities of Fisher 344 rats grew exclusively on the mesenterium to form a solid mass (11, 12). We therefore chose the RCN-9 cell line to establish a suitable novel rat model with clinicopathological features that mimic PET.

Correspondence to: Motohiro Imano, MD, Ph.D., Department of Surgery, Kinki University Faculty of Medicine, 377-2 Ohno-higashi Osaka-Sayama, Osaka 589-8511, Japan. Tel: +81 73660221, Fax: +81 723683382, e-mail: imano@med.kindai.ac.jp

Key Words: Peritoneal carcinomatosis, rat model, mesothelial cells, submesothelial layer, RCN-9 cells, fibroblast.

## Materials and Methods

**Animals.** Adult male Fischer 344 rats (eight weeks of age, weighing 155-180 g) obtained from SLC Japan (Shizuoka, Japan) were maintained at 22°C under a 12:12-h light-dark cycle, and had access to food and water *ad libitum*. All experiments were conducted with the approval of the Institutional Animal Experimentation Committee of Kinki University.

**Cells.** The RCN-9 tumor cell line, which was established from Fischer 344 rat colon carcinoma cells (9), was purchased from the Riken Cell Bank (Tsukuba, Japan). The cells were cultured in RPMI-160 medium (Gibco BRL, Grand Island, NY, USA) supplemented with 10% heat-inactivated fetal bovine serum at 37°C in 5% CO<sub>2</sub>.

**Development of model. Novel PC model:** Rats were anesthetized by intraperitoneal injection of pentobarbital (50 mg/kg). The abdominal skin was cleaned and disinfected. A 1-cm midline incision starting 4.5 cm below the xiphoid was used to open the upper abdomen. Using a mosquito clamp, the peritoneum was held gently and the entire peritoneum was scraped twenty times using a sterile cotton swab (Figure 1a). The abdomen was then closed with a single-layer 3-0 vicryl interrupted suture; 1×10<sup>6</sup> RCN-9 cells in 1 ml phosphate-buffered saline were injected into the peritoneal cavity of each rat using an 18-gauge needle.

**Scrape model:** In the scrape group, the scraping step described above was performed without RCN-9 cell injection.

**Control model:** In the control group, RCN-9 cells were injected without the scraping step described above.

**Experimental design.** To clearly observe the progressive development of PC, euthanasia was performed at 1, 3, 5, 7, 10, 12, 14, or 21 day(s) after surgery in each group (n=5 at each time point, total n=120).

The abdomen was opened through a midline incision from the xiphoid to the scrotal region. Right and left dorsal incisions were made at the cranial and caudal edges, allowing the abdomen to be opened in the manner of double doors. After inspecting the intra-abdominal organs, the peritoneum was obtained (Figure 1b).

**Hematoxylin and eosin staining.** The freshly-obtained peritonea were fixed in 4% paraformaldehyde, dehydrated in graded alcohol, and routinely embedded in paraffin. Four-micrometer sections were processed for routine hematoxylin and eosin staining.

**Measurement of tumor and submesothelial layer thickness.** An image of the measured area was captured using a CCD camera (ACT-2U; Nikon Corporation, Tokyo, Japan), and the thickness of tumor and the submesothelial layer in each image was traced and measured by computer. RCN-9 tumor thickness was defined as the distance between the surface and the deepest portion of the tumor. The thickness of the submesothelial layer was defined as the distance between the mesothelial cell layer and the outer layer of the muscle.

**Statistical analyses.** Statistical analyses were performed using Stat View® (SAS Institute Inc., Cary, NC, USA). Student's *t*-test was used to analyze the difference between the novel PC model and the scrape model. The Pearson product moment was used to analyze the

association between the thickness of RCN-9 cell layer and the length of time following RCN-9 cell injection. A value of *p*<0.05 was considered significant.

## Results

**Macroscopic findings. Control model:** At 1, 3, 5, 7, 10, and 12 day(s), no changes were observed in the peritoneum. However, at 14 and 21 days, a small metastatic nodule was observed only at the RCN-9 cell injection site in the peritoneum. No other metastatic nodules were present in the other sites (Figure 2a).

**Scrape model:** The scrape model showed no macroscopic change at any time throughout our investigation.

**Novel PC model:** At days 1, 3, and 5, no changes were seen in the peritoneum. However, at day 7, a thin peritoneal membrane metastasis was observed (Figure. 2b). At 14 days, the peritoneal metastasis had grown thicker, in a manner similar to PC of PET (Figure 2c), and small metastatic nodules were observed at the mesentery (Figure 2d). At day 21, peritoneal metastases exhibited irregularly shaped formations; we observed a peritoneum coated by tumor and bloody ascites.

**Microscopic findings. Control model:** In the control model, no changes to the mesothelial cells or the sub-mesothelial layer were observed at any time point (Figure 3a). At days 14 and 21, a small RCN-9 nodule was observed only at the injection site.

**Scrape model:** At day 1, mesothelial cells appeared to peel-off, exposing the basement membrane. Remnant mesothelial cells exhibited a cuboidal cytoplasm and spherical nuclei with mild atypism, thus appearing to be activated mesothelial cells. Connective tissue was observed in the submesothelial layer (Figure 3b). The submesothelial layer thickness was seen to increase gradually from day 3, maximizing at day 10, and subsequently decreasing (Figure 4a).

**Novel PC model:** At day 1, we observed the same changes as found in the scrape model in mesothelial cells and the submesothelial layer (Figure 3c). However, in the submesothelial layer, edematous changes and loose fibroblasts were seen; the submesothelial layer had thickened to an average of 44.1 μm (Figure 3c). RCN-9 cells were adherent at day 1; growth was thus observed only on the exposed basement membrane and not in the region of mesothelial cells (Figure 3d).

At day 3 and day 5, RCN-9 cells exhibited growth and the submesothelial layer thickness increased. At day 7, fibroblasts increased, and the submesothelial layer achieved a maximum thickness of an average of 418.7 μm (Figure 4a and 5a). RCN-9 cells grew to the peritoneal surface and reached the muscle layer (Figure 5b).

At day 21, RCN-9 cell thickness plateaued at a maximum average diameter of 3512.3 μm and invaded muscle tissue

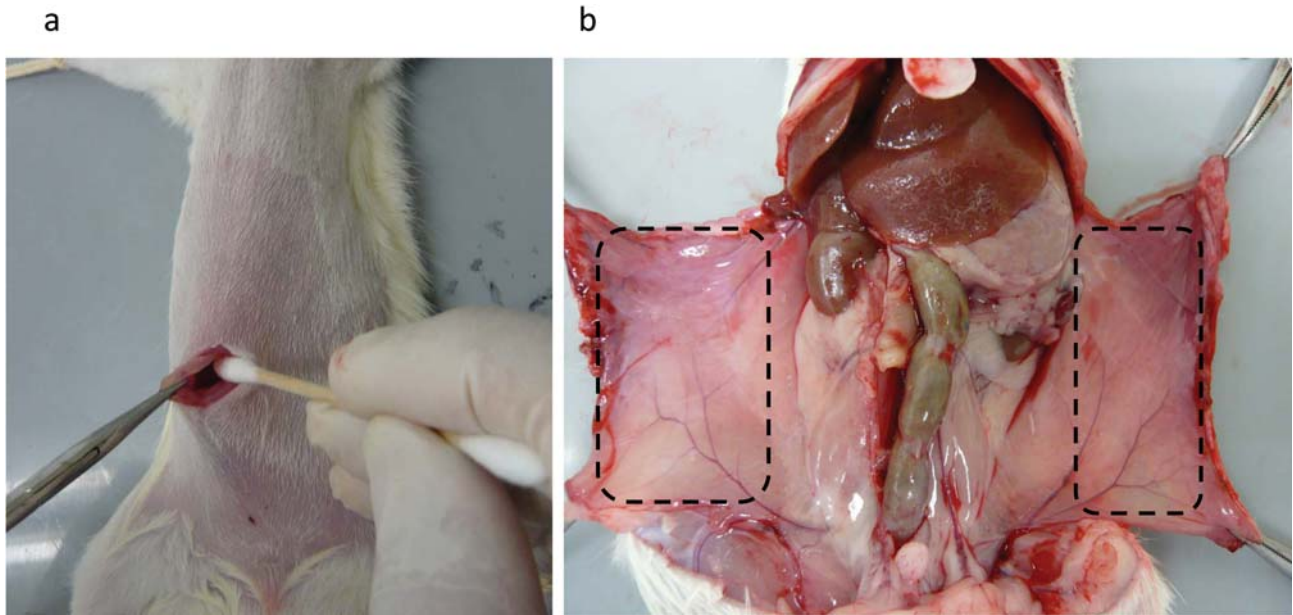


Figure 1. Development of a rat peritoneal carcinomatosis model. a: Method for scraping of the peritoneum. The peritoneum was held with a mosquito clamp and scraped with sterile cotton in a fan-like fashion. b: The abdomen was opened with two flaps, similar to double doors.

(Figure 4b and 5c). However, the population of fibroblasts in the submesothelial layer decreased; the submesothelial layer was reduced to an average thickness of 53.4  $\mu\text{m}$ ; mesothelial cells, as observed on day 1, appeared to be activated mesothelial cells (Figure 4a and 5d).

There was a significant positive correlation between the thickness of the RCN-9 cell layer and the length of time after RCN-9 cell injection ( $R^2=0.898$ ;  $p<0.01$ , Figure 4b). In contrast, the submesothelial layer thickness maximized during the early phase of RCN-9 cell growth and diminished over the subsequent 10 days, in contrast to the increase in RCN-9 cell layer thickness; at day 21, the submesothelial layer was about as thick as the one observed at the start of the experiment (Figure 4a).

On each day, there was a significant difference between the thickness of the submesothelial layer of the novel PC model and the scrape model (Figure 4a,  $p<0.05$ ).

## Discussion

Yashiro *et al.* investigated the relationships among carcinoma cells, submesothelial layer and fibroblasts (13, 14). Yao *et al.* and Suh *et al.* also described the effects of cytokine up-regulation by myofibroblasts on mesothelial cells (15-17). Although these studies were *in vitro*, in previously established animal PC models, including mouse and rat models, PC lesions appeared as tumor nodules, which were not present in the peritoneum. The omentum and mesentery, which easily form PC as tumor nodules, are thin membranes

in which changes in the submesothelial layer and fibroblasts are difficult to investigate. Our novel animal model establishes PC in the peritoneum. This is the first report of a animal model of PC for PET.

Although previous studies described injecting  $1 \times 10^7$  RCN-9 cells into peritoneal cavities, they did not report RCN-9 cells growing on the peritoneum (11, 12). When we injected  $1 \times 10^6$  RCN-9 cells into the peritoneal cavity in the present study, peritoneal metastasis occurred only at the injection site in the control model. However, in the novel PC model, which included localized cell scraping, metastasis occurred in the peritoneum in an early phase, and RCN-9 cells coated the peritoneum in the late phase. Additionally, we showed there to be a significant positive correlation between the thickness of RCN-9 cell layer and the length of time following RCN-9 cell injection. These results indicate that RCN-9 cells are invasive to muscle, over a sufficient length of time, similar to clinical experience, implying that we successfully established a novel rat model for PET. By peeling-off mesothelial cells, we potentially created an environment that allowed for metastasis of RCN-9 cells on the peritoneum to occur easily.

The mechanism underlying mesothelial adhesion of cancer cells has been widely investigated. Adhesion of cancer cells to the mesothelial layer is mediated by several adhesion molecules; many are also expressed by endothelial cells (18). Therefore, mesothelial cells are thought to play an important role in PC. From our findings, RCN-9 cells were not adherent in the control model, and were adherent only in areas lacking



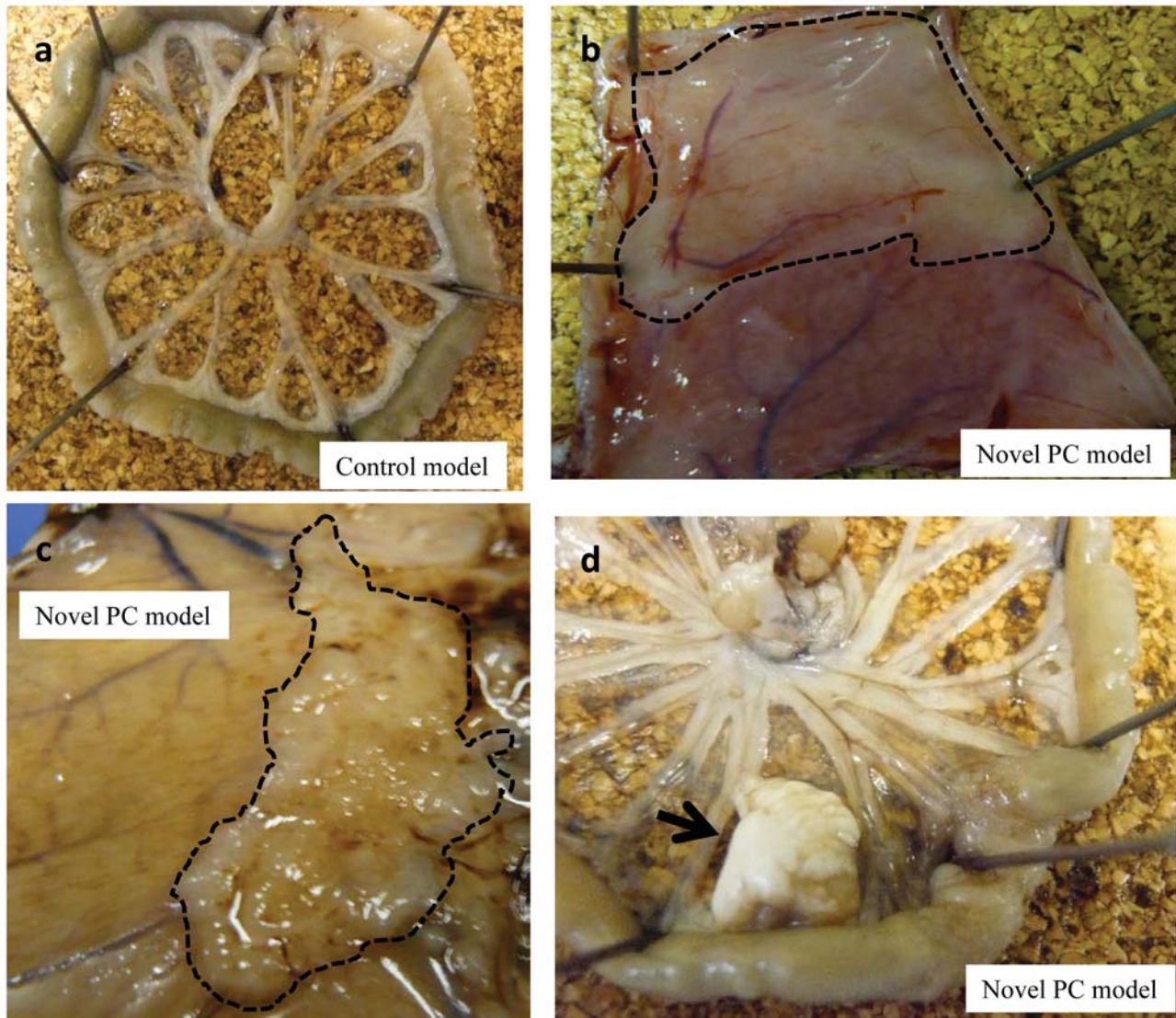


Figure 2. Macroscopic findings of control and novel peritoneal carcinomatosis model. a: Control model at day 1. No metastatic nodules were observed in the mesentery. b: Novel PC model at day 7. Peritoneal metastasis was observed as a thin white membrane (dot enclosed). c: Novel PC model at day 14. A mat of white, uneven peritoneal metastasis was observed in the peritoneum (dot enclosed). d: Novel PC model at day 14. A small white nodule was observed in the mesentery (arrow).

mesothelial cells in the novel PC model. Therefore, we hypothesized that mesothelial cells act to prevent the adhesion of cancer cells. Sharma *et al.* reported that pleural mesothelial cells express a sialomucin complex to prevent the adherence of ovarian cancer cells to the pleura (19). Heath *et al.* showed FAS-dependent apoptosis of cultured human mesothelial cells to be induced by AW480 colorectal tumor cells, and concluded that mesothelial cells acted as a barrier to tumor cell adherence to the submesothelial layer (20). Our data agree with these observations.

Additionally, thickening of the submesothelial layer occurred at initial phases of the novel PC and scrape models—more so in

the novel PC model, in which the submesothelial layer thickening grew particularly quickly at first. These results underscore the relationship between fibroblasts, cancer invasion and cancer stroma (21, 22). Although fibroblasts within the stroma help to create an environment permissive for tumor growth, angiogenesis, and invasion (22, 23), there are few reports concerning fibroblasts in the submesothelial layer. We have shown that the submesothelial layer thickness increases in the initial phase following RCN-9 cell injection.

An imageable fluorescent model of metastasis using tumor cells injected into a living green fluorescent protein (GFP) animal model would be very useful (24). However, to

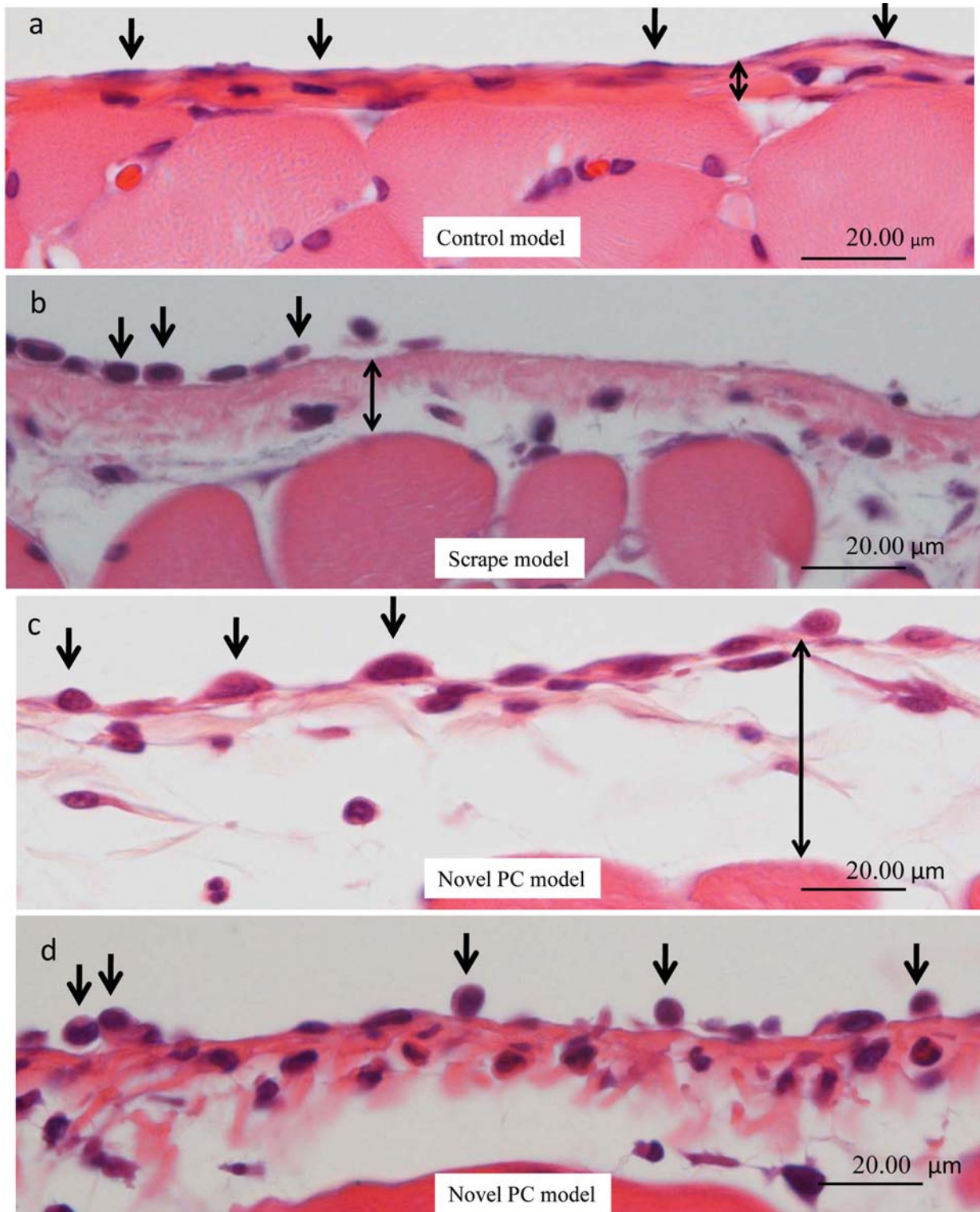


Figure 3. Microscopic findings of control, scrape and novel peritoneal carcinomatosis. a: Control group at day 21. Flat mesothelial cells with small nuclei were observed on the mesothelium (arrow). A thin, tight submesothelial layer was observed (double arrow). b: Scrape model, at day 1. Mesothelial cells on the peritoneum exhibited cuboidal cytoplasm and spheroidal nuclei (arrow). In the submesothelial layer, connective tissue was observed (double arrow). c: Novel PC model, at day 1. Mesothelial cells exhibited the same changes of the scrape model (arrow) and edematous change were present in the submesothelial layer (double arrow). d: Novel PC model at day 1. RCN-9 cells (arrow) were adherent to the basement membrane in the region in which mesothelial cells had peeled-off.

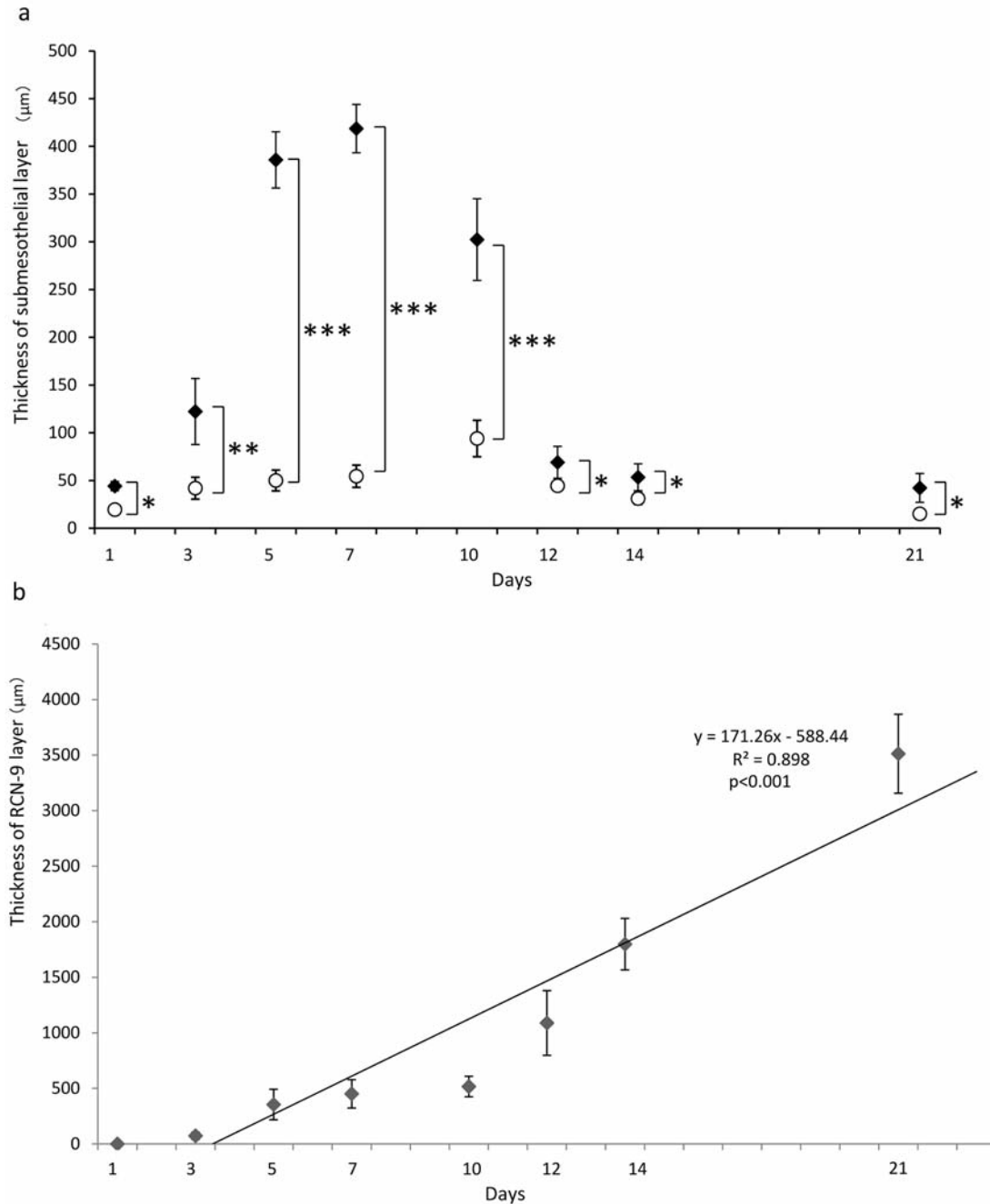


Figure 4. Thickness of submesothelial layer and RCN-9 cell layer. *a*: Submesothelial cell layer thickness in the novel peritoneal carcinomatosis model increased in the early phase (day 7) of tumor growth. In the late phase, the submesothelial cell layer thickness decreased to the level observed at day 1. There were significant differences between the novel PC and scrape models at each time point. \* $p < 0.05$ ; \*\* $p < 0.01$ ; \*\*\* $p < 0.001$ ;  $n = 5$ . *b*: RCN-9 cell layer thickness increased with time, and there was a positive correlation between the thickness and length of time after RCN-9 cell injection ( $R^2 = 0.898$ ;  $p < 0.001$ ).

investigate changes in the submesothelial layer and fibroblasts, histological examination would be needed in order to obtain material after sacrifice. Therefore, real-time optical imaging is probably impossible.

While the role played by submesothelial layer fibroblasts in the establishment of PC remains unclear, our study indicates that it is potentially critical and warrants further investigation.



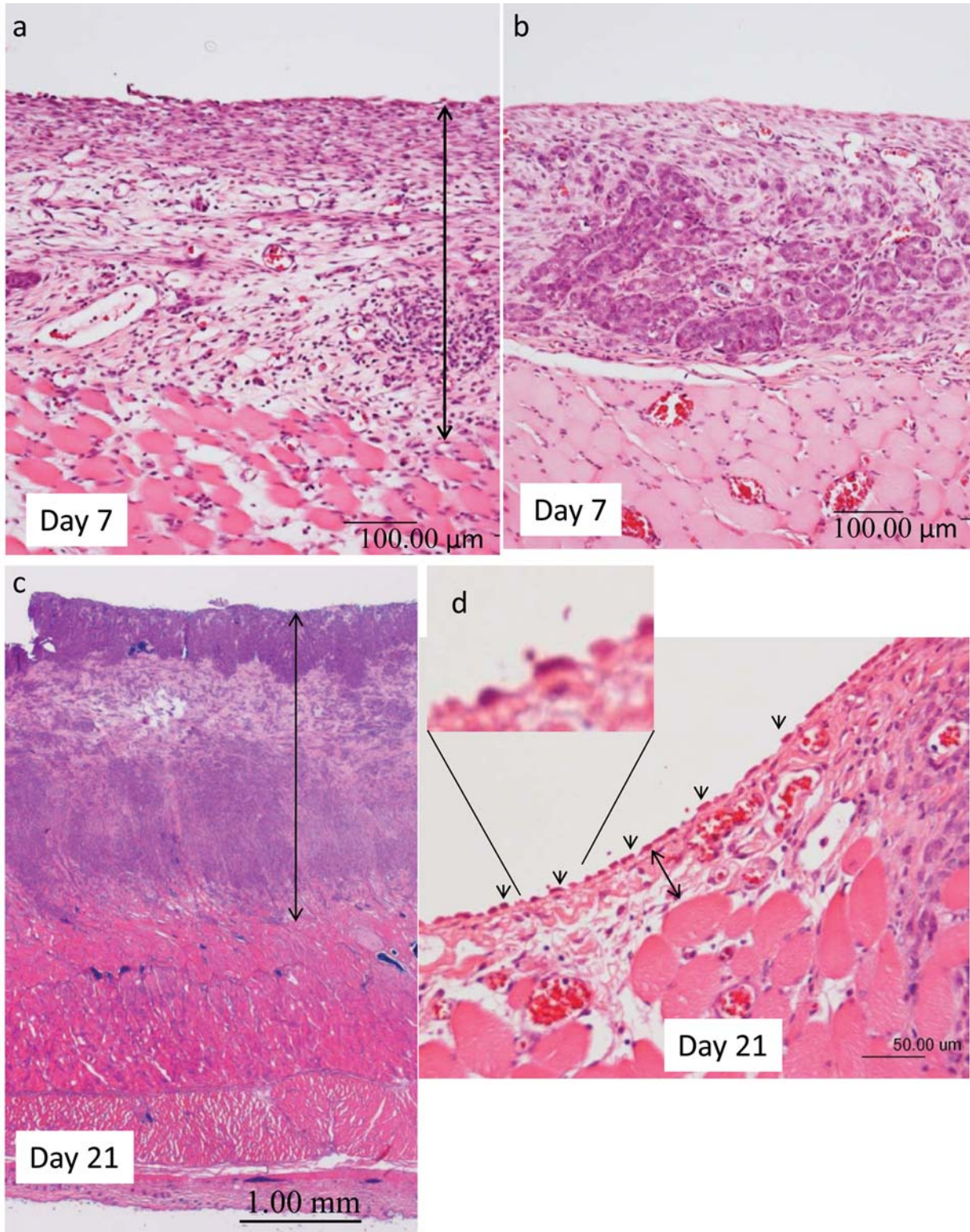


Figure 5. Microscopic findings of the novel peritoneal carcinomatosis model at day 7 and 21. a: The thickness of the mesothelial layer reached a maximum at day 7 in the novel PC model (double arrow). b: Day 7 in the novel PC model. RCN-9 tumor had grown, reaching the muscle layer. c: Day 21 in the novel PC model. The RCN-9 tumor cells had invaded the muscle tissue, and the thickness of the RCN-9 cell layer reached a maximum average diameter of 3512.3  $\mu\text{m}$  (double arrow). d: The thickness of the submesothelial layer decreased to an average of 53.4  $\mu\text{m}$  (double arrow) and was similar to that at day 1. Fibroblasts in the submesothelial layer decreased, and mesothelial cells exhibited the activated form (arrow, inset higher power).

# Acknowledgements

The Authors express their appreciation to Dr. Harumasa Ohyanagi, Vice Board Director of the University of KinDAI Himeji, for his expert comments on the manuscript. Additionally, we thank Ms. Fusako Kamada, Mr. Shigeaki Yamanaka, Mr. Kentaro Egawa, Mr. Nobuyuki Mizuguchi, and Mr. Shinsuke Watanabe for their technical assistance.

# References

- 1 Sadeghi B, Arvieux C, Glehen O, Beaujard AC, Rivoire M, Baulieux J, Fontaumard E, Brachet A, Caillot JL, Faure JL, Porcheron J, Peix JL, Francois Y, Vignal J and Gilly FN: Peritoneal carcinomatosis from non-gynecologic malignancies: Results of the EVOCAPE 1 multicentric prospective study. *Cancer* 88: 358-363, 2000.
- 2 Al-Shammaa HA, Li Y and Yonemura Y: Current status and future strategies of cytoreductive surgery plus intraperitoneal hyperthermic chemotherapy for peritoneal carcinomatosis. *World J Gastroenterol* 14: 1159-1166, 2008.
- 3 Shirouzu K, Isomoto H, Morodomi T, Ogata Y, Akagi Y and Kakegawa T: Primary linitis plastica carcinoma of the colon and rectum. *Cancer* 74: 1863-1868, 1994.
- 4 Isobe Y, Nashimoto A, Akazawa K, Oda I, Hayashi K, Miyashiro I, Katai H, Tsujitani S, Kodera Y, Seto Y and Kaminishi M: Gastric cancer treatment in Japan: 2008 annual report of the JGCA Nationwide Registry. *Gastric Cancer* 14: 301-316, 2011.
- 5 Furukawa H, Hiratsuka M, Iwanaga T, Imaoka S, Ishikawa O, Kabuto T, Sasaki Y, Kameyama M, Ohigashi H, Nakamori S and Yasuda T: Extended surgery -left upper abdominal exenteration plus Appleby's method- for type 4 gastric carcinoma. *Ann Surg Oncol* 4: 209-214, 1997.
- 6 Iwasa S, Nakajima TE, Nakamura K, Takashima A, Kato K, Hamaguchi T, Yamada Y and Shimada Y: First-line fluorouracil-based chemotherapy for patients with severe peritoneal disseminated gastric cancer. *Gastric Cancer* 15: 21-26, 2011.
- 7 Li PC, Chen LD, Zheng F and Li Y: Intraperitoneal chemotherapy with hydroxycamptothecin reduces peritoneal carcinomatosis: results of an experimental study. *J Cancer Res Clin Oncol* 134: 37-44, 2008.
- 8 Klaver YL, Hendriks T, Lomme RM, Rutten HJ, Bleichrodt RP and de Hingh IH: Intraoperative hyperthermic intraperitoneal chemotherapy after cytoreductive surgery for peritoneal carcinomatosis in an experimental model. *Br J Surg* 97: 1874-1880, 2010.
- 9 Inoue Y, Kashima Y, Aizawa K and Hatakeyama K: A new rat colon cancer cell line metastasizes spontaneously: Biologic characteristics and chemotherapeutic response. *Jpn J Cancer Res* 82: 90-97, 1991.
- 10 Song E, Chen J, Ouyang N, Wang M, Exton MS and Heemann U: Kupffer cells of cirrhotic rat livers sensitize colon cancer cells to Fas-mediated apoptosis. *Br J Cancer* 84: 1265-1271, 2001.
- 11 Suzuki T, Yanagi K, Ookawa K, Hatakeyama K and Ohshima N: Blood flow and leukocyte adhesiveness are reduced in the microcirculation of a peritoneal disseminated colon carcinoma. *Ann Biomed Eng* 26: 803-811, 1998.
- 12 Yanagi K and Ohshima N: Angiogenic vascular growth in the rat peritoneal disseminated tumor model. *Microvasc Res* 51: 15-28, 1996.
- 13 Yashiro M, Chung YS, Inoue T, Nishimura S, Matsuoka T, Fujihara T and Sowa M: Hepatocyte growth factor (HGF) produced by peritoneal fibroblasts may affect mesothelial cell morphology and promote peritoneal dissemination. *Int J Cancer* 67: 289-293, 1996.
- 14 Yashiro M, Chung YS, Nishimura S, Inoue T and Sowa M: Fibrosis in the peritoneum induced by scirrhous gastric cancer cells may act as 'soil' for peritoneal dissemination. *Cancer* 77: 1668-1675, 1996.
- 15 Yao Q, Qu X, Yang Q, Wei M and Kong B: CLIC4 mediates TGF-beta1-induced fibroblast-to-myofibroblast transdifferentiation in ovarian cancer. *Oncol Rep* 22: 541-548, 2009.
- 16 Yao Q, Cao S, Li C, Mengesha A, Kong B and Wei M: Micro-RNA-21 regulates TGF-beta-induced myofibroblast differentiation by targeting PDCD4 in tumor-stroma interaction. *Int J Cancer* 128: 1783-1792, 2011.
- 17 Suh KS, Crutchley JM, Koochek A, Ryscavage A, Bhat K, Tanaka T, Oshima A, Fitzgerald P and Yuspa SH: Reciprocal modifications of CLIC4 in tumor epithelium and stroma mark malignant progression of multiple human cancers. *Clin Cancer Res* 13: 121-131, 2007.
- 18 Bracke ME: Role of adhesion molecules in locoregional cancer spread. *Cancer Treat Res* 134: 35-49, 2007.
- 19 Sharma RK, Mohammed KA, Nasreen N, Hardwick J, Van Horn RD, Ramirez-Icaza C and Antony VB: Defensive role of pleural mesothelial cell sialomucins in tumor metastasis. *Chest* 124: 682-687, 2003.
- 20 Heath RM, Jayne DG, O'Leary R, Morrison EE and Guillou PJ: Tumour-induced apoptosis in human mesothelial cells: a mechanism of peritoneal invasion by FSA ligand/FAS interaction. *Br J Cancer* 90: 1437-1442, 2004.
- 21 Imano M, Okuno K, Itoh T, Ishimaru E, Satou T and Shiozaki H: Increased osteopontin-positive macrophage expression in colorectal cancer stroma with synchronous liver metastasis. *World J Surg* 34: 1930-1936, 2010.
- 22 Gaggioli C, Hooper S, Hidalgo-Carcedo C, Grosse R, Marshall JF, Harrington K and Sahai E: Fibroblast-led collective invasion of carcinoma cells with differing roles for RhoGTPases in leading and following cells. *Nat Cell Biol* 9: 1392-1400, 2007.
- 23 Kalluri R and Zeisberg M: Fibroblasts in cancer. *Nat Rev Cancer* 6: 392-401, 2006.
- 24 Bouvet M, Wang J, Nardin SR, Nassirpour R, Yang M, Baranov E, Jiang P, Moossa AR and Hoffman RM: Real-time optical imaging of primary tumor growth and multiple metastatic events in a pancreatic cancer orthotopic model. *Cancer Res* 62: 1534-1540, 2002.

Received December 12, 2012

Revised March 4, 2013

Accepted March 4, 2013